

## Augmented fuzzy logic inertial response for hybrid microgrid

Somesh Bhattacharya; Brian Azzopardi; Sukumar Mishra

Published in:

Proceedings of The 12th Mediterranean Conference on Power Generation, Transmission, Distribution and Energy Conversion (MEDPOWER 2020)

Publication date:

November 2020

Document Version

Peer reviewed version

Citation for published version (IEEE format):

S. Bhattacharya, B. Azzopardi, S. Mishra, "Augmented fuzzy logic inertial response for hybrid microgrid", in the Proceedings of The 12th Mediterranean Conference on Power Generation, Transmission, Distribution and Energy Conversion (MEDPOWER 2020), 2020. DOI: 10.1049/icp.2021.1270.

### General rights:

Copyright and moral rights for the publications made accessible in the public portal are retained by the authors and/or other copyright owners and it is a condition of accessing publications that users recognise and abide by the legal requirements associated with these rights.

Personal use of this material is permitted. Permission from the copyright owner of the published version of this document must be obtained for all other uses, in current or future media, including distribution of the material or use for any profit-making activity or for advertising/promotional purposes, creating new collective works, or reuse of any copyrighted component of this work in other works.

You may freely distribute the URL/DOI identifying the publication in the public portal.

### Policy for disabling free access:

If you believe that this document breaches copyright please contact us at [energy@mcast.edu.mt](mailto:energy@mcast.edu.mt) providing details, and we will remove access to the work immediately and investigate your claim.

# AUGMENTED FUZZY LOGIC INERTIAL RESPONSE FOR HYBRID MICROGRID

*Somesh Bhattacharya<sup>1\*</sup>, Brian Azzopardi<sup>1,2</sup>, Sukumar Mishra<sup>3</sup>*

<sup>1</sup> MCAST Energy Research Group, Institute of Engineering and Transport,  
Malta College of Arts, Science, and Technology (MCAST), Paola, Malta

<sup>2</sup> Azzopardi and Associates Firm, International

<sup>3</sup> Department of Electrical Engineering, Indian Institute of Technology Delhi, India  
[\\*Somesh.Bhattacharya@mcast.edu.mt](mailto:*Somesh.Bhattacharya@mcast.edu.mt)

**Keywords:** MICROGRIDS, INERTIAL RESPONSE, DROOP CONTROL

## Abstract

Hybrid microgrids inertia controls have been dependent on rotating sources as reference for the frequency control for the network in the islanded mode. However, with the increasing share of static sources outnumbering the former type of generation, and the high R/X ratio of the interconnecting lines due to which proportional power sharing is hampered, the control strategy demands an augmentation. This paper proposes an inertial response strategy using the Takagi-Sugeno (T-S) Fuzzy logic based derivative control for the hybrid microgrids where static sources such as Photovoltaic systems (PVs) and the interlinking converters (ICs) lead the stability reference of the network followed by rotating sources, and the latter is also responsible for the proportional load sharing along with the static sources. The simulations performed on the hybrid microgrid demonstrate the efficacy of the proposed T-S Fuzzy logic based derivative controller for inertial response over the conventional proportional-derivative (P-D) controller, where the latter is generally used for obtaining an inertial response.

## 1 Introduction

The global solar energy yield has increased by 60% in the last decade, and owing to that, the share of energy storage technology has also seen an increasing trend with 40% rise in the past decade [1]. However, such large static interconnections with the utility grid invites several issues related with frequency, apart from the more serious problem of voltage regulation. The most important being the reduction in the inertia. The IEEE-1547-2018 interoperability standards [2] state that distributed energy resources (DERs) should participate in the frequency support as a part of the ancillary service provision without disconnecting from the grid during any abnormal operation.

The problem of inertia control by emulating the synchronous generator characteristics have been studied in [3-6]. However, all the aforementioned papers limited their research to power electronics/ voltage source inverter (VSI) based devices and their dynamics related to power sharing and inertia emulation.

The issue of virtual inertia in the presence of rotating sources such as diesel generators (DGs) was discussed in [7], in which a frequency support approach was discussed for PV based VSI based on DC link voltage ( $V_{dc}$ ) control along with de-loading from the PVs. However, the DG was considered to be operating in the constant power factor operation, and system behavior in the grid connected mode was also not considered in the paper.

The application of T-S fuzzy logic control in multi-machine power systems for controlling active and reactive powers was demonstrated in [8], from which the idea of the application of the aforementioned logic for frequency-proportional control was emanated.

This paper explores the capability of static sources participating in providing inertial response in presence of DG. In order to mitigate the frequency overshoot or undershoot and to enhance the transient response of the VSI, A TS-Fuzzy logic based inertial response method is formulated, instead of the conventional P-D controller. Simulations have been performed on the hybrid microgrid in the grid connected mode, and the transition from the aforementioned mode to the islanded mode. It is shown through the simulations that the proposed control can help in providing frequency response and also help in transferring from the grid connected mode to the isolated mode, without the need of a derivative droop control, which was subject to constrained parameter sensitivity when seen from the dynamic stability point of view.

The paper is organized as follows: The description of the system considered is briefed in section 2. The control strategy for the static and the rotating sources is formulated in section 3. Section 4 discusses the various cases on which the system is simulated, and section 5 concludes the paper.

## 2 System Considered

A DC microgrid coupled to an AC system is considered in this paper. The sources which comprise of the DC microgrid include battery based energy storage devices and a PV, and all the DC based DERs are coupled to a common DC bus. The DC bus is coupled to an IC which provides the necessary frequency regulation and response services to the utility grid. The nominal voltage at the DC bus is  $800V_{dc}$ . Further, the inverter generates or absorbs active and reactive power at  $400V_{ac}$ . The PV in the DC microgrid is a constant dispatch source and produces a constant active power, therefore the DC link voltage is maintained constant at the PV- DC bus.

The DC microgrid comprises of three battery based energy storage (BESS) which are located at separate busses through resistive cables. The charging and the discharging of the

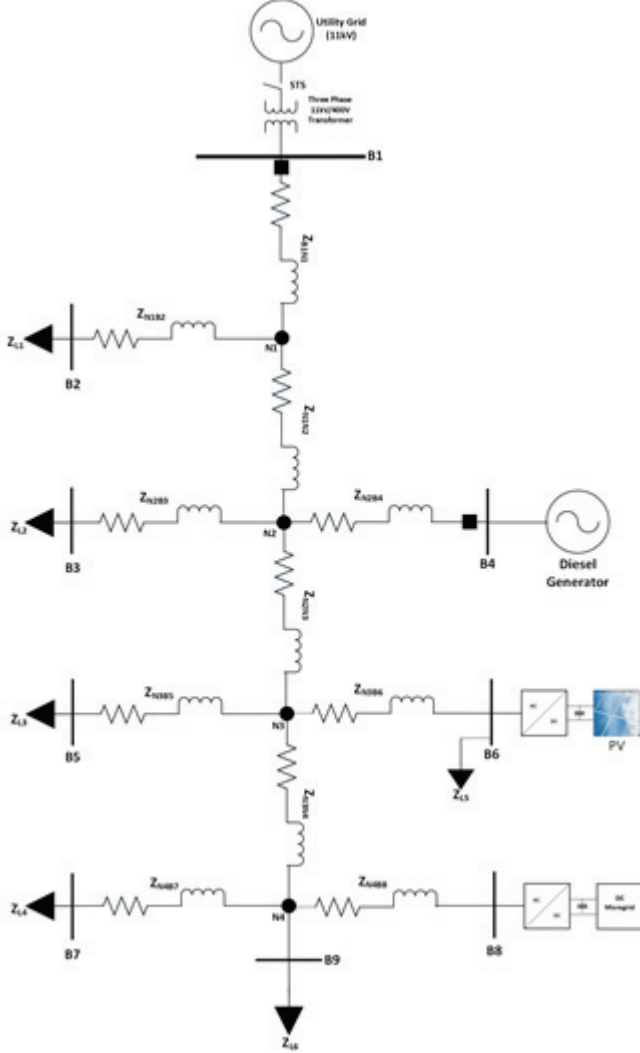


Fig.1. Single line diagram of the hybrid microgrid

BESS units are decided by the active power reference set by IC. The reactive power to be delivered or absorbed is dependent on the power factor at which the inverter operates. Therefore, it is intended that the inverter operates as a P-Q bus. However, in case of a grid event which involves a frequency sag or swell.

In this paper, the BESS is not considered dormant (energy delivery for peak levelling and power smoothening), and is as assumed to actively participate in the energy delivery or absorption. The SoC based sharing ensures that the BESS which have a higher SoC share more powers than the one having a lower SoC. Lithium Ion batteries have been considered in this work, although they are costlier than the conventional lead acid batteries, the former have a prolonged life cycle if the SoC criteria are respected.

### 3 Control strategy

#### 3.1 Control of the DC microgrid

As mentioned in the preceding section, the DC microgrid, coupled with the AC sub-grid consists of PV and BESS. Constant impedance based loads are considered thus the power flow from the DC microgrid can be briefed as in (1).

$$P_{IC} = \sum_{i=1}^3 P_{BESS,i} + P_{PV} + P_{grid} \quad (1)$$

In this equation,  $P_{IC}$  is the active power of the interlinking converter,  $P_{PV}$  denotes the power of the PV on the DC side,  $P_{BESS}$  is individual battery power which is delivered or absorbed according to the reference power set by the AC grid and the DC loads. The PV is held at its MPPT with the help of a DC boost converter, and the BESS is controlled with the help of bidirectional DC-DC converters. Droop based power sharing (2) is employed for the DC voltage regulation in the batteries, which also ensure sharing of powers in accord with their respective SoCs. The droop control is based on the DC power measurements as opposed to the current measurements, which are the general convention used for the droop control within a DC power system. The droop control has the reference voltage,  $V_{dc,ref}$  as the output and  $P_{BESS}$  and the individual state of charge,  $SoC_i$  as the inputs in percentage.

$$V_{dc,ref} = \begin{cases} V_{dc0} - m_d \cdot P_{BESS} \cdot e^{-SoC_i}; \forall SoC \in (20,100) \\ V_{dc0} - m_c \cdot P_{BESS} \cdot (e^{SoC_i} - 1); \forall SoC \in (0,20) \end{cases} \quad (2)$$

In the equation,  $V_{dc0}$  denotes the nominal DC link voltage, which is the intended voltage at the common DC bus.  $m_d$  and  $m_c$  denote the droop coefficients for discharging and charging respectively. When the DC microgrid is islanded from the AC sub system, the charging or the discharging of the individual battery depends upon the DC loading during that time and the PV insolation level. The PV in the DC microgrid operates at its MPPT at all times, the duty cycle of which is controlled with the help of a DC boost converter.

The inner control loops for the bidirectional converters for the BESS comprise of the current and the voltage controllers. The outer voltage regulator of the converter is responsible for maintaining the DC link voltage, whereas the current controller generates the pulse width modulated (PWM) references for the converter switches, as well as improve the dynamic response of the converter.

#### 3.2 Control of the AC side of the system

A distributed control is designed for the DERs to operate in both the grid connected and the isolated modes. The constant power control for the DERs is modified in such a way that the inertial response parameter is added to the control system. The power regulation is achieved by regulating  $V_{dc}$ , and the output of the resultant reference  $V_{dc}$  produced is compared with the output voltage of the static DER to generate the current references. To emulate the inertial response in the DERs, the swing equation can be deliberated as-

$$2H \frac{d\Delta\omega}{dt} = \Delta P_m - \Delta P_e - D_\omega (\Delta\omega) \quad (3)$$

In (3), the parameters  $H$ ,  $\omega$ ,  $P_m$ ,  $P_e$  and  $D_\omega$  denote the inertia constant, speed, mechanical and electrical powers respectively, and the damping coefficient. The active power or the DC power can be expressed as a function of the DC link voltage, in terms of the power loss component. The further assumptions are positioned on the fact that in the grid connected mode, the quadrature, 'q'-axis voltage is zero and only the direct, 'd' axis voltage exists, hence,  $V_{dc} \cdot I_{dc} = 1.5 V_d \cdot I_d$ , as seen at the inverter output, and therefore, (4) can be written in terms of  $V_{dc}$  as under-

$$\frac{V_{dc,ref}^2 - V_{dc}^2}{R_l} = (Ms + D)\Delta\omega \quad (4)$$

In this Equation,  $R_l$  is an approximated load resistance term, which can be expressed as a tuning coefficient. Which when multiplied by the 'M' and the 'D' terms will give an equivalent value of the inertia and damping coefficients,  $M_e$  and  $D_e$  respectively. Therefore, (4) can be reframed as-

$$V_{dc,ref}^2 - V_{dc}^2 = (M_e \cdot s + D_e)(\omega - \omega_0) \quad (5)$$

In this equation, the inertial response parameter,  $\Delta\omega$  is therefore passed through an equivalent derivative controller to mimic the inertial response in the grid connected mode. The resultant of this outer control is therefore treated as an auxiliary signal to the DC link voltage control. Let  $y_0$  be the value of the aforementioned signal, therefore,

$$y_0 = (M_e s + D_e) \cdot (\omega_{ref} - \omega) \quad (6)$$

In this equation,  $\omega_{ref}$  is the reference frequency setting in the grid connected mode, which is thereby compared with the frequency sensed by the phase locked loop (PLL). The new value of the  $V_{dc,ref}$  can therefore be shown in the equation below-

$$V_{dc,ref}^2 = V_{dc,ref}^2 - y_0 \quad (7)$$

This signal is therefore compared with the actual DC link voltage, with the help of a PI compensator. The equivalent control signal is therefore added with the power reference, which is also a function of the resultant inertia control. The auxiliary power signal can be defined as under-

$$y_{00} = \frac{P_{ref} - D_e \cdot (\omega - \omega_0)}{V_d} \quad (8)$$

This signal,  $y_{00}$  is therefore added to the compensated output of the voltage controller, and therefore, in order to achieve the requisite current references, the decoupled PI control based current controller is used, which will further deliver the gate pulses to the inverter circuitry. The rest of the governing

equations for the inverter control, as mentioned in the theory above are deliberated in (9), (10) and (11).

$$(V_{dc,ref}^2 - V_{dc}^2) \left( \frac{K_{pvdc} \cdot s + K_{ivdc}}{s} \right) = I_{d\Delta,ref} \quad (9)$$

$$I_{d\Delta,ref} + y_{00} = I_{id,ref} \quad (10)$$

$$V_{id} = (I_{id,ref} - I_{id}) \left( \frac{K_{pc} \cdot s + K_{ic}}{s} \right) - \omega L I_{iq} \quad (11)$$

### 3.3 Control of the rotating generators

The active distribution network, which can also be termed as a grid connected microgrid, has one DG rated 8100VA. The presence of this DG introduces some complexities: When the system enters the isolated mode, the DG will attempt to govern the system frequency, and for the static DERs to participate in the frequency regulation along with the DGs, the latter have to be embedded with an inertia control feature. In this work, however, an alternate approach is followed, in which the static DERs remain in the power control mode, while providing frequency response, as in the grid connected mode, and the DG frequency and the voltage controllers are modified in order to share the active and reactive powers with the DC microgrid, as the PV continues to operate in the MPPT mode. The reference frequency and the voltage generated for the DG is hence a function of both active and reactive power as can be seen in (12) and (13).

$$\omega_{dg,ref} = \omega_0 - m_p \cdot ((P_{dg} - P_{dg,ref}) - K_p \cdot (Q_{dg} - Q_{dg,ref})) \quad (12)$$

$$V_{dg,ref} = V_0 - n_q \cdot ((Q_{dg} - Q_{dg,ref}) + K_q \cdot (P_{dg} - P_{dg,ref})) \quad (13)$$

The overall transfer function can be seen in Fig.2, which shows the small signal model of the AVR of the DG, where  $K_a$ ,  $K_e$  and  $K_f$  are the AVR, exciter and the damper gains respectively, whereas the coefficients  $T_a$ ,  $T_e$ ,  $T_{do}'$  and  $T_f$  are the time constants associated with the AVR, exciter, generator and the damper of the AVR. The DG governor is modeled as a third order system, and the transfer functions with the time constants,  $T_g$  and  $T_{ch}$  denoting the governor and the re-heater time constants respectively.  $T_d$  denotes the exponential time delay introduced because of the dead time of the diesel engine [7]. The resultant transfer function of the governor setup is a third order function. In general, the governor has an inverse P-f droop characteristic, i.e. the power references are produced based on the deviation, and the same is also called the primary frequency control. In this case, however, as the governor has both active and reactive powers as inputs, the aforementioned time constants are treated as tunable parameters, and a small signal analysis has been performed for the DG system, in order to achieve the optimum droop control parameters for proper power sharing between the DG and the DC microgrid.



Based on the linearized small signal equations of the machine, as can be seen in the input-output relations of the transfer function seen in Fig.2.

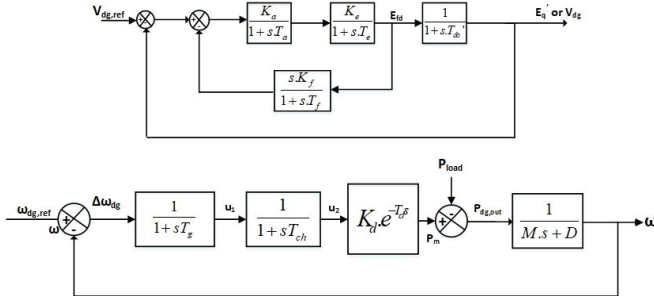


Fig.2. Transfer function for the DG

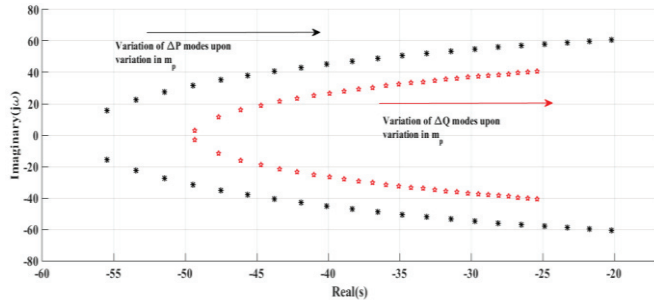


Fig.3. Variation in the \$\Delta P\$ and \$\Delta Q\$ modes when the droop coefficient, \$m\_p\$ is varied.

The small signal stability of the modified control is analyzed, and the Eigen value plot can be seen in Fig.3. It was seen that by varying the droop coefficient, \$m\_p\$, and the two modes which are excited upon the variation are the \$\Delta P\_{dg}\$ and \$\Delta Q\_{dg}\$ modes, as shown in the figure. It can be observed, when \$m\_p\$ was increased from 0.005 p.u. to 0.02 p.u., the frequency of oscillation is increased from 3.18Hz to 9.54Hz for the \$\Delta P\_{dg}\$ mode, and the former parameter showed an increasing trend for the same variation from 0.8Hz to 6.3Hz. Therefore, in a DG, the absence of the first order filter introduces low frequency modes of oscillations.

### 3.3 T-S Fuzzy Logic Control

The DERs achieve inertial response through a derivative (P-D) control, as mentioned in the previous sub-section. The P-D control, however introduces significant noise in the system upon entering the isolated mode, which can also deteriorate the stability of the system. The T-S fuzzy controller consists of antecedents and consequents upon which the rule base are constructed. The former helps in the creation of the fuzzy rule base, and the consequents are the outcome of the fuzzy rule base, which helps in attaining several gain variations. To achieve inertial response, the frequency and the deviation in the frequency have been chosen as the inputs, which are to be fuzzified. The fuzzification of the inputs are performed with the help of membership functions, which exist for both positive and negative sets. The error functions to be fuzzified at the \$k^{th}\$ sample can be seen in (14) and (15).

$$e_1(k) = \omega_{ref}(k) - \omega(k) \quad (14)$$

$$e_2(k) = e_1(k) - e_1(k-1) \quad (15)$$

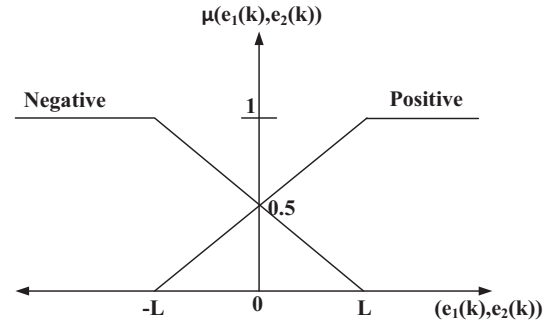


Fig.4. Membership functions of the T-S fuzzy logic control

The membership functions can hence be formulated in (16) as-

$$\begin{aligned} \mu_p(x_i) &= \begin{cases} \frac{x_i + L}{2L}, & -L < x_i < L \\ 1, & x_i \leq -L \\ 0, & x_i \geq L \end{cases} \\ \mu_n(x_i) &= \begin{cases} \frac{-x_i + L}{2L}, & -L < x_i < L \\ 0, & x_i \leq -L \\ 1, & x_i \geq L \end{cases} \end{aligned} \quad (16)$$

Here, \$\mu\_p\$ and \$\mu\_n\$ denote the positive and negative membership functions, and the value of \$x\_i\$ are the error dynamic equations, \$e\_1(k)\$ and \$e\_2(k)\$. The parameter, \$L\$ is the length of the slope within which the membership function is active. For both the above mentioned membership functions, the upper and the lower limits are set to 1 and 0, since the value of the membership functions cannot exceed unity. The plot for the membership function can be shown in Fig.4. The rule base when the controller is fuzzified linguistically can be defined in four sets, which can be seen (17), (18), (19) and (20).

When \$e\_1(k)\$ is positive and \$e\_2(k)\$ is positive,

$$u_1(k) = K_1 \cdot (a_1 \cdot e_1(k) + a_2 \cdot e_2(k)) \quad (17)$$

When \$e\_1(k)\$ is positive and \$e\_2(k)\$ is negative,

$$u_2(k) = K_2 \cdot (K_1 \cdot (a_1 \cdot e_1(k) + a_2 \cdot e_2(k))) \quad (18)$$

When \$e\_1(k)\$ is negative and \$e\_2(k)\$ is positive,

$$u_3(k) = K_3 \cdot (K_1 \cdot (a_1 \cdot e_1(k) + a_2 \cdot e_2(k))) \quad (19)$$

When \$e\_1(k)\$ is negative and \$e\_2(k)\$ is negative,

$$u_4(k) = K_4 \cdot (K_1 \cdot (a_1 \cdot e_1(k) + a_2 \cdot e_2(k))) \quad (20)$$

The values, \$u\_1\$, \$u\_2\$, \$u\_3\$ and \$u\_4\$ represent the fuzzified output of the controller. In order to de-fuzzify the set of outputs obtained, the Zadeh's rules are applied and the control output, \$u(k)\$ can be obtained from (20)

$$u(k) = \frac{\sum_{j=1}^4 (\mu_j(k))^\alpha \cdot u_j(k)}{\sum_{j=1}^4 (\mu_j(k))^\alpha} \quad (20)$$

## 4 Results and Discussions

### 4.1 Operation in the grid connected mode

The base case scenario for the hybrid AC-DC microgrid is presented in this sub-section. Initially, the PV is operating at its MPPT and the interlinking converter follows a fixed power reference of -5kW.

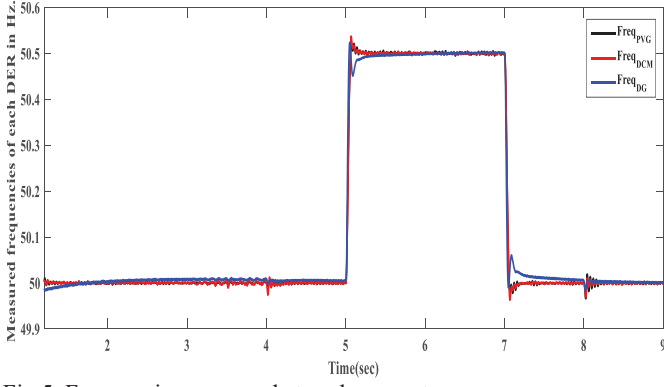


Fig.5. Frequencies measured at each generator

A condition arises during grid interconnection, when the grid sees a frequency rise of 0.5Hz at the 5<sup>th</sup> sec for 2 seconds. The IC and the PV respond to this change in frequency by reducing their active powers.

Fig.5. shows the measured frequency at the output of PV, IC and the DG respectively. The events which are simulated are as follows: The insolation of the PV at the AC side of the microgrid network was reduced by 25% at the 4<sup>th</sup> sec; Frequency rise at the grid PCC was simulated from the 5<sup>th</sup> sec to the 7<sup>th</sup> sec; A load change of 4kW was observed at the 8<sup>th</sup> sec at bus 9.

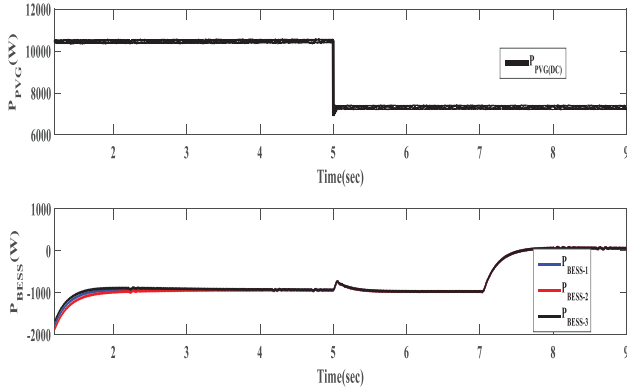


Fig.6. Powers measured at the DC microgrid

As can be seen in Fig.6, the PV in the DC microgrid generates around 10.2kW, and the three BESS units absorb 1000W in the power sharing mode. Following this, a change in the PV power at the AC side at the 4<sup>th</sup> sec does not bring any change or transient in the DC system of the DC microgrid, as the system is connected to the grid and the DC microgrid is connected at a separate PCC.

At the 5<sup>th</sup> sec, it is seen that the PV power of the DC microgrid is reduced following a reduction in the insolation by 30%. However, it is also observed that the reduction of 3000W is taken up by the sources present in the DC microgrid only. It is also to be noted that the grid frequency swell is recorded at the same time (refer Fig.5) and since in accord with the inertial droop setting,  $D_e$  which is produced by the T-S fuzzy controller, the increase in frequency leads to a further absorption of active power by the IC of the DC microgrid by 3100W, and therefore, no appreciable change is visible in the BESS powers. However, at the 7<sup>th</sup> sec, when the grid frequency is retained at its nominal value, the BESS power is automatically increased as the DC side of the PV

continues to operate at its new MPPT, i.e. at a reduced insolation.

Fig.7. shows the active powers of the PV and the IC. It is observed that in the grid connected mode, the PV operates at its MPPT, and the IC works at the instructed power reference. During the frequency swell, the PV keeps operating at its MPPT, as a much higher droop coefficient is chosen for the PV, which does not result in an appreciable change in the PV power. The change in the DG power upon the change in frequency has been shown in Fig.8. It is seen that the droop coefficients,  $m_p=0.02$  p.u. and  $n_q=0.03$  p.u. bring out a reduction of 2000W in the DG when the frequency is reduced by 0.5 p.u.

#### 4.2 Transition from the grid connected to the isolated mode

In the grid connected mode, the PV and the IC operate in the fixed power operation, as discussed in the previous section. However, when the microgrid enters the isolated mode, the PV still operates in the MPPT, and the DC microgrid along with the DG has the responsibility of controlling the voltage and frequency of the entire system.

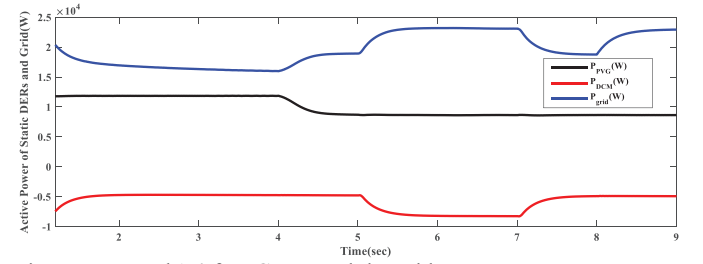


Fig.7. Measured 'P' for IC, PV and the grid.

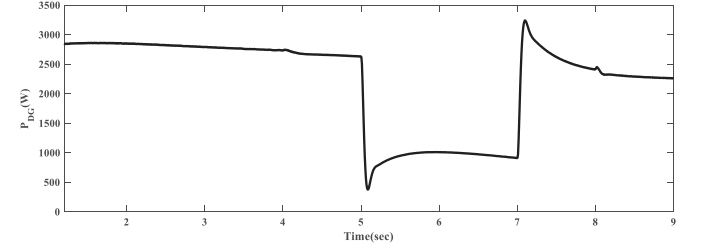


Fig.8. Active power output of the DG.

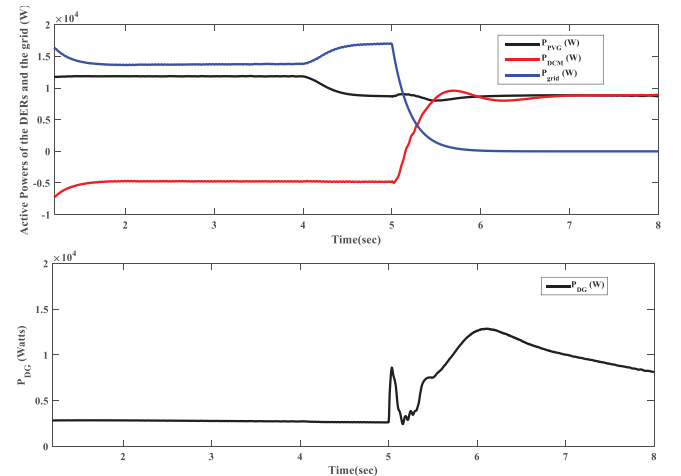


Fig.9. Active powers of the static, rotating DERs and the grid during grid transition

It can be seen in Fig.9 that the PV insolation is reduced at the 4<sup>th</sup> sec. Following the loss of the grid at the 5<sup>th</sup> sec, the active power of the IC is increased from -5kW to 9kW, while the PV remains at its MPPT, with the same reduced insolation. It can be observed that even with a change of 14kW in the isolated mode, especially in a low voltage system, the system retains its stability. The power delivered by the DG during the mode transition can be seen in the same figure. The DG settles at a power of 8kW, i.e. a power increase of 6kW was performed after the microgrid enters the isolated mode.

The reactive powers measured at the PV and IC outputs are shown in Fig.10. It is observed that since the PV is operating at its MPPT, the power factor is kept at unity, therefore, the reactive power of the PV is maintained at 0 in both grid connected and the isolated modes respectively. The reactive power measured at the IC, however, operates at a leading power factor, as the reactive power is dependent on the generated active power, and since the DC microgrid absorbs active power, even keeping a power factor command of 0.95 makes the IC to absorb a reactive power of 1800VAr. At the 5<sup>th</sup> sec, as soon as the system enters isolation, the reactive power generated by the IC is positive, as the latter VSI based source generates active power.

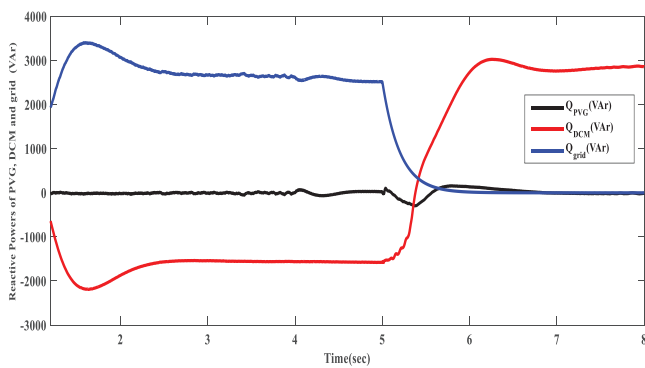


Fig.10. Response of the reactive powers of the static sources under mode transition

The performance comparison for the frequency response between the P-D control for inertial response and the proposed T-S fuzzy based controller is shown in Fig.11.

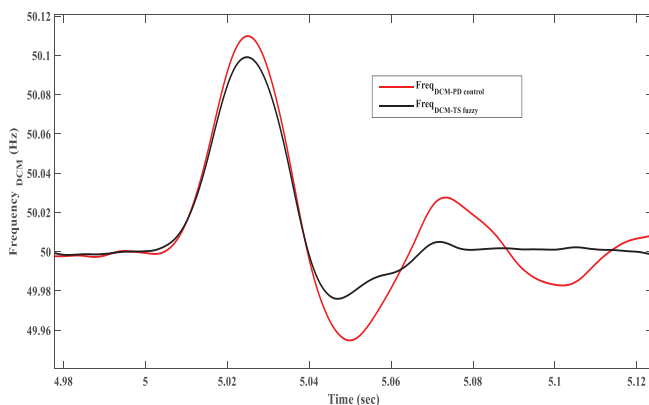


Fig.11. Comparison between the frequency responses with T-S Fuzzy logic controller and P-D controller

As can be seen from the figure, the overshoot in the frequency is decreased by 4%, and the settling time also decreases by 0.2 seconds.

## 5 Conclusions

For the proposed hybrid microgrid topology entering the islanded mode of operation, the T-S fuzzy logic based control augments the inertial response, as measured at the IC. The overshoot was decreased and the settling time was significantly improved by virtue of the aforementioned control. It was also observed that the modified control for the DG plays an important role in the frequency response in the grid connected mode of operation.

## 6 Acknowledgements

This work was supported in part by the EU Commission H2020 TWINNING projects namely JUMP2Excel (Joint Universal Activities for Mediterranean PV Integration Excellence) and NEEMO (Networking for Excellence in Electric Mobility Operations) under grants 810809 and 857484 respectively.

## 7 References

- [1] 'Energy Storage', <https://greentechmedia.com/articles>, accessed June 2020
- [2] IEEE Std. 1547<sup>TM</sup>-2018: 'IEEE Standard for Interconnection and Interoperability of Distributed Energy Resources with Associated Electric Power Systems Interfaces, 2018
- [3] Panda, R.K., Mohapatra, A., Srivastava, S.C.: 'Enhancing inertia of solar photovoltaic-based microgrid through notch filter based PLL in SRF control, IET Gener. Transm. Distrib., 14(3), Jan. 2020., pp. 379-388.
- [4] Liu, J., Miura, Y., Bevrani, H., Ise, T.: 'Enhanced virtual synchronous generator control for parallel inverters in microgrids', IEEE Trans. Smart Grid., 8(5), Feb. 2016., pp. 2268-2277.
- [5] Chowdhury, A., Liang, X., Xhang, H.: 'Fuzzy secondary controller based virtual synchronous generator control for microgrids', In Proc. IEEE Indl. Appl. Society Annual Meeting, Cincinnati, USA, Oct. 2017, pp.1-14.
- [6] Fang, J., Li, H., Tang, Y., Blaabjerg, F.: 'On the inertia of future more-Electronics power systems', IEEE Access, 7(4), Oct. 2018, pp. 2130-2146.
- [7] Lyu, X., Xu, Z., Zhao, J., Wong, K.P.: 'Advanced frequency support strategy of photovoltaic system considering changing working conditions, IET Gener. Transm. Distrib., 12(2), Feb. 2018., pp. 363-370.
- [8] Mishra, S., Dash, P.K., Panda, G.: 'TS-fuzzy controller for UPFC in multi-machine power system', IET Gener. Transm. Distrib., 14(1), Jan. 2000., pp. 15-22.